This is an open access article published under an ACS AuthorChoice License, which permits copying and redistribution of the article or any adaptations for non-commercial purposes.

ACS OMEGA

Article

Cite This: ACS Omega 2019, 4, 1443−1448

http://pubs.acs.org/journal/acsodf

Hierarchically Porous Silica Prepared with Anionic Polyelectrolyte−Nonionic Surfactant Mesomorphous Complex as Dynamic Template

Chengxiang Shi,[†] Huan Wang,[†] Qiulin Bi,[†] Liqing Li,[†] Pingchuan Sun,[‡,§] and Tiehong Chen*[,†,§]

[†]Institute of New Catalytic Materials Science, School of Materials Science and Engineering, Key Laboratory of Advanced Energy Materials Chemistry (MOE), Nankai University, Tianjin 300350, PR China

[‡]Key Laboratory of Functional Polymer Materials of Ministry of Education, College of Chemistry, Nankai University, Tianjin 300071, PR China

[§]Collaborative Innovation Center of Chemical Science and Engineering (Tianjin), Tianjin 300071, PR China

Supporting Information

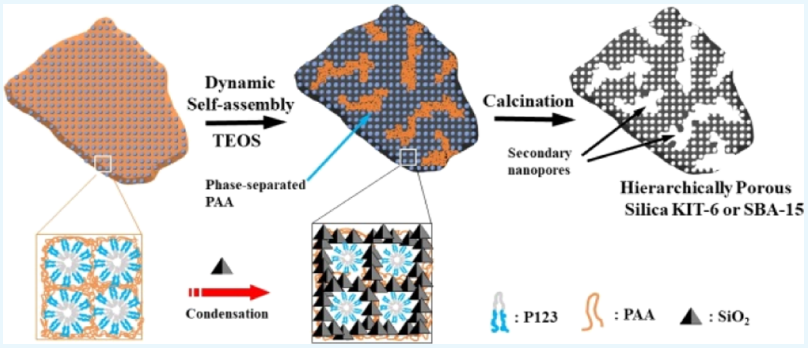

ABSTRACT: Hierarchically porous silica KIT-6 and SBA-15 mesostructures were successfully synthesized by using a mesomorphous complex of a nonionic triblock copolymer (pluronic P123) and an anionic polyelectrolyte (polyacrylic acid) as the dynamic template. The obtained mesoporous silica materials possessed both ordered mesopores (∼7 nm) and nanopores (∼15−50 nm), and the long-range order of the mesophase was not perturbed by the embedded larger secondary nanopores. Moreover, hierarchically porous silica KIT-6 exhibited enhanced adsorption capacity in enzyme and protein immobilization, which was attributed to the hierarchically porous structure.

INTRODUCTION

Hierarchically porous materials can be applied in diverse fields and have been widely studied.[1,2] In general, hierarchically porous materials possess interconnected porosity at different length scales, large surface area, excellent permeability and storage properties, and all these structural characters are important for the loading and diffusion of substances, endowing them with important applications in the fields of catalysis, adsorption, separation, and biomedicine.[3−9]

In recent decades, hierarchically porous materials have been prepared by different methods, including soft or hard template method, post-treatment, acid treatment, freeze-drying, phase separation, and so forth.[2,10−16] Hierarchically porous materials could be prepared with soft templates, but it is always hard to achieve simultaneous regulation of the order and interconnection of the pore structure because of the difficulty in controlling the cooperation of different templates.

In nature, some inorganic materials produced by organisms possess complex morphologies as well as hierarchically porous structures.[17] For instance, sea urchin spines (made of $CaCO_3$ crystals) exhibit a porous morphology and meanwhile remain single-crystalline. The formation process of the "porous" single crystals of biominerals is dynamically controlled by a complex organic matrix generated time-dependently.[18] Inspired by the formation mechanism of biominerals, our research group recently reported a new method to synthesize hierarchically porous, single-crystalline silica colloids with anionic polyelectrolytes/cationic surfactants as the dynamic template.[19] Because of the ionic self-assembly between anionic polyelectrolytes and cationic surfactants, a highly ordered mesomorphous polyelectrolyte-surfactant complex could form. During the synthesis, negatively charged silica precursors were directed by the liquid crystal complex template and an ordered mesostructure was obtained; meanwhile, the electrostatic interaction between polyelectrolyte chains and surfactant micelles was disturbed or disassembled. Some of polyelectrolyte chains were phase-separated from the complex to form chain domains, which acted as templates for the secondary nanopores within the synthesized materials after calcination. The polyelectrolyte−surfactant mesomorphous complex

Received: December 19, 2018
Accepted: January 2, 2019
Published: January 16, 2019

© 2019 American Chemical Society

DOI: 10.1021/acsomega.8b03565
ACS Omega 2019, 4, 1443−1448

(PSMC) templating method has become a general approach to prepare hierarchically porous materials, including hierarchically porous silica,[20−25] PMO,[20] carbon,[26] and titanium phosphate,[27] with different mesomorphous phases and morphologies.

So far, in the PSMC templating methods reported in the literature, only cationic surfactants were used to form complexes with anionic polyelectrolytes via electrostatic interaction. However, the size of the ordered mesopore was about 3 nm because of the relatively small size of the cationic surfactant micelles.[28] The low-cost and nontoxic nonionic surfactants have exhibited advantages as templates in the preparation of mesostructured materials. For instance, the triblock copolymer, P123, is a very popular template for the synthesis of mesoporous silica SBA-15 and KIT-6, whose mesopore size is generally larger than 6 nm.[29] Herein, we extend the PSMC templating method to the category of nonionic surfactants. Through hydrogen-bonding interaction, the anionic polyelectrolyte (PAA) and nonionic surfactant (P123) can also form a mesomorphous complex,[30−32] which can be used as the dynamic template to prepare hierarchically porous silica KIT-6 (cubic $Ia\bar{3}d$ mesostructure) and SBA-15 (2D hexagonal *P6mm* mesostructure). These materials exhibited well-ordered mesopores (∼7 nm) as well as larger secondary nanopores (∼15−50 nm). Interestingly and importantly, the long-range order of KIT-6 and SBA-15 was not influenced by the presence of secondary nanopores, that is, the hierarchically porous KIT-6 and SBA-15 exhibited a single crystalline mesostructure, but with embedded larger nanopores. The hierarchically porous silica KIT-6 exhibited enhanced adsorptive capacity of biomacromolecules.

RESULTS AND DISCUSSION

In the synthesis procedure, immediately after the addition of concentrated HCl to the solution containing P123/PAA, flocculent sediment was observed. This is because the hydrogen bonding between PAA and PEO segments of P123 was enhanced by the addition of HCl.[30] The precipitated PAA/P123 complex was collected and submitted to small-angle X-ray diffraction (XRD) analysis. As shown in Figure S1, the high-intensity diffraction peak at $2\theta = 0.94°$ indicated that the complex possessed a well-ordered mesostructure, though the mesomorphous phase could not be clearly identified, probably because of the variation of water content in the complex during the collection and measurement. The transmission electron microscopy (TEM) images (Figure S2) of the PAA/P123 complex showed that the morphology of the complex colloids was irregular. Meanwhile, there were ordered mesophases shown in the images, which corresponds to the mesostructure in the XRD pattern of the PAA/P123 complex.

After the addition of tetraethyl orthosilicate (TEOS), the assembly of silica precursors was directed by the PAA/P123 mesomorphous complex. ^{13}C CP/MAS NMR spectra (Figure S3) of the as-synthesized samples confirmed that both PAA and P123 existed. Small-angle XRD spectra of the calcined samples are shown in Figure 1a−d, and all the patterns showed two distinct diffraction peaks in the range of $2\theta = 1.0−1.2°$. The expanded XRD patterns of PAA-0 and PAA-0.2 displayed four resolved diffraction peaks in the small range of $2\theta = 1.4−2.2°$. Besides the (211) and (220) diffraction peaks, there also appeared (321), (400), (420), and (332) diffractions of the cubic $Ia\bar{3}d$ mesostructure, indicating that the obtained materials were all KIT-6. For samples of PAA-0.4 and PAA-0.5, the diffraction peaks at $2\theta = 1.4−2.2°$ were slightly less resolved, and this is due to the increasing of the secondary nanopores as discussed in the following.

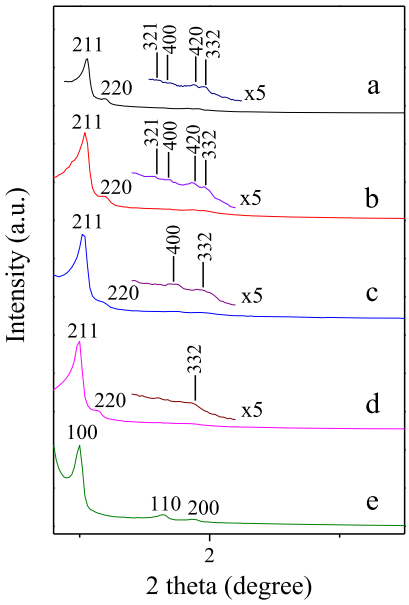

Figure 1. Small-angle XRD patterns of the calcined samples (a) PAA-0, (b) PAA-0.2, (c) PAA-0.4, (d) PAA-0.5, and (e) HCl-5.0.

The scanning electron microscopy (SEM) image (Figure S4) of the typical KIT-6 mesoporous silica (PAA-0.5) synthesized with the PAA/P123 complex template exhibited the morphology of irregular micrometer-sized particles, which could inherit from the morphology of the PAA/P123 complex template (Figure S2). TEM images of the samples PAA-0, PAA-0.5, and HCl-5.0 are shown in Figure 2. For the sample synthesized without PAA (PAA-0), only highly ordered single-modal mesopores could be observed (Figure 2a). However, for

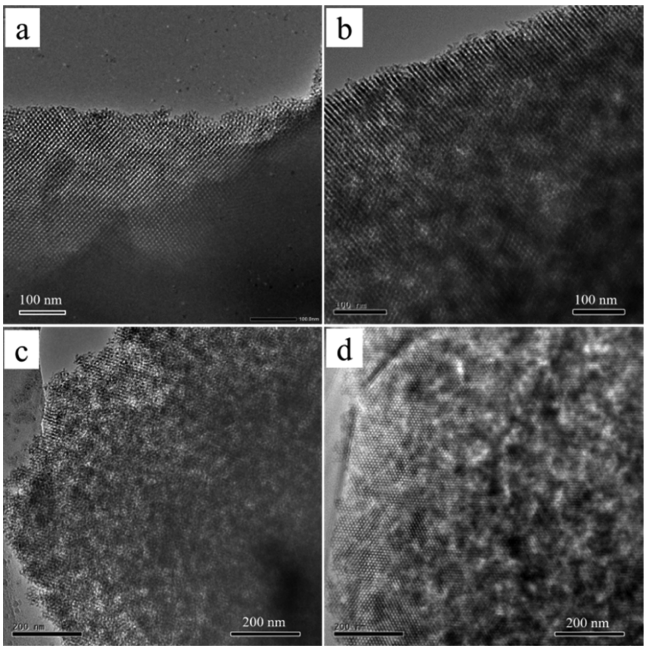

Figure 2. TEM images of the calcined samples (a) PAA-0, (b,c) PAA-0.5, and (d) HCl-5.0.

DOI: 10.1021/acsomega.8b03565
ACS Omega 2019, 4, 1443−1448

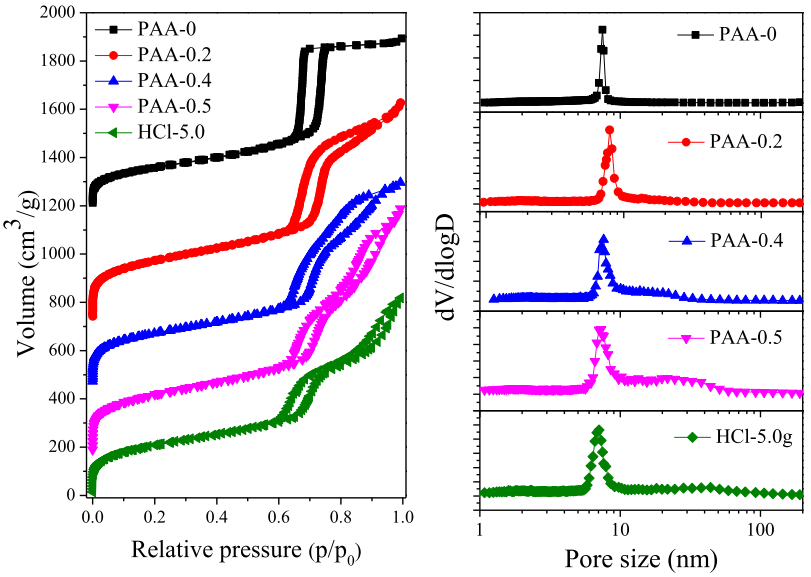

Figure 3. Nitrogen adsorption−desorption isotherms and pore size distribution curves of the calcined samples PAA-0, PAA-0.2, PAA-0.4, PAA-0.5, and HCl-5.0.

Table 1. Textural and Structural Parameters of Calcined Samples

sample	d^a/nm	BET surface area/m^2 g^{-1}	mesopore size/nm	secondary nanopore size/nm	total volume^b/cm^3 g^{-1}
PAA-0	8.40(d_{211})	717	7.5		1.02
PAA-0.2	8.48(d_{211})	822	7.9	15−20	1.37
PAA-0.4	8.65(d_{211})	825	7.6	15−30	1.42
PAA-0.5	8.82(d_{211})	847	7.3	15−50	1.56
HCl-5.0	8.82 (d_{100})	736	7.1	20−60	1.26

^{a}Calculated from the position of diffraction peaks. ^{b}Calculated from p/p_0 = 0.98 with the BET method.

the samples synthesized with PAA, besides the highly ordered mesopores, there appeared heterogeneous contrasts of light and dark inside, indicating the presence of secondary nanopores within the matrix of the highly ordered mesoporous structure (Figure 2b−d). The overall long-range order of the mesostructure remained well even with the embedded secondary nanopores, indicating a single crystalline mesostructure.

The nitrogen adsorption desorption isotherms of the samples are shown in Figure 3. Without addition of PAA, the sample PAA-0 exhibited a typical type IV isotherm. The adsorption step at p/p_0 of 0.7−0.8 corresponded to a sharp peak at 7.5 nm in the pore size distribution curve (Figures 3 and S5). However, for the samples of PAA-0.2, PAA-0.4, and PAA-0.5, there appeared two obvious adsorption steps at p/p_0 of about 0.7−0.8 and 0.8−0.95 in adsorption branches, respectively. The first step was due to nitrogen capillary condensation in the ordered mesopores of KIT-6 and gave rise to a sharp peak at ∼7.5 nm. With the increasing amount of PAA in the synthesis, the second adsorption step became more and more pronounced. For the sample prepared with 0.5 g PAA, the second adsorption step at about p/p_0 = 0.8−0.95 corresponded to a broad peak at ∼15−50 nm, which was due to the secondary nanopores templated by phase-separated PAA domains, and this was consistent with the results shown in the TEM images.

As shown in Table 1, it could be found that with the increasing amount of PAA, the d value (d_{211}) increased, while the order mesopore size decreased, indicating that the mesopore wall became continuously thicker, which would lead to better hydrothermal stability.

According to the literature,[33] in the synthesis of mesoporous silica templated by P123, the mesostructure could be tuned by the amount of HCl. Here, in our synthesis, while the amount of concentrated HCl was increased to 5.0 g, the synthesized sample became 2D hexagonal *P6mm* mesostructured SBA-15 (Figure 1e). Both the TEM image (Figure 2d) and the nitrogen adsorption isotherms (Figure 3, HCl-5.0) showed that SBA-15 templated by PAA/P123 also exhibited a hierarchically porous single-crystalline mesostructure.

On the basis of the characterizations, the formation process of hierarchically porous KIT-6 and SBA-15 particles was sketched. As shown in Scheme 1, first, the anionic polyelectrolyte (PAA) and nonionic surfactants (P123) formed

Scheme 1. Formation Mechanism of Hierarchically Porous Silica KIT-6 or SBA-15 Templated by the PAA/P123 Complex

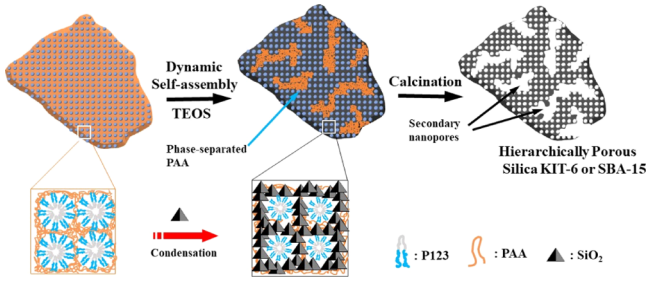

DOI: 10.1021/acsomega.8b03565
ACS Omega 2019, 4, 1443−1448

mesomorphous complexes through hydrogen-bonding interaction. Upon the addition of TEOS, the hydrolyzed silicate ions interacted with P123 micelles, thus the hydrogen bonding interactions between P123 and PAA would be dismantled. As a result, some PAA chains were phase-separated from the PAA/P123 complex, which could act as the templates for the interstitial nanopores inside the KIT-6 or SBA-15 particles.

As reported in the literature, multimodal porous materials exhibited advantages in bioimmobilization.[20,34] Here, to test the bioimmobilization capacity of the obtained hierarchically porous silica, PAA-0.5 was used as the typical example in the immobilization of lysozyme and bovine serum albumin (BSA). Figure 4 presented the adsorption curves of PAA-0 and PAA-0.5 in the lysozyme solution. The adsorption amount of lysozyme on the two samples is listed in Table 2. Obviously, for PAA-0.5, the adsorption rate was greatly faster than that of PAA-0. The adsorption capacity of PAA-0 and PAA-0.5 reached 378 and 436 mg g^{-1}, respectively. In the adsorption of BSA, whose molecular size (40 Å × 40 Å × 140 Å) is bigger than that of lysozyme (19 Å × 25 Å × 43 Å), as listed in Table 2, the immobilized amount of BSA was approximately 175 mg g^{-1} onto PAA-0.5, and this value was larger than that on PAA-0 (115 mg g^{-1}). The higher immobilized amount on PAA-0.5 was attributed to the hierarchically porous structure.

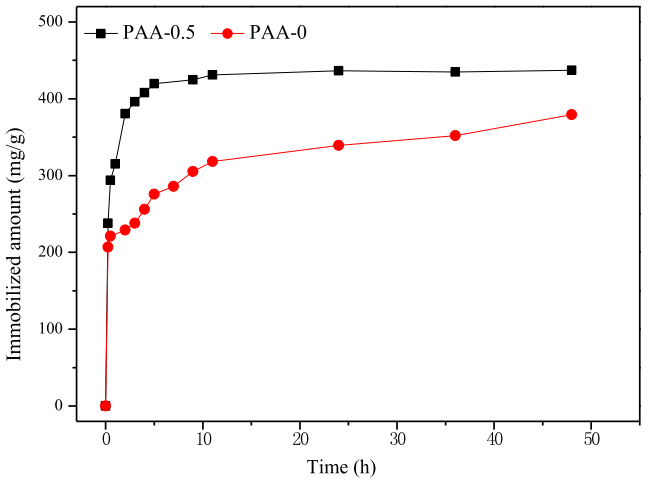

Figure 4. Lysozyme immobilization rate on PAA-0 and PAA-0.5.

Table 2. Enzyme and Protein Adsorption on Single-Modal and Hierarchically Porous KIT-6

			enzyme immobilized amount/mg·g^{-1}	
enzyme	molecular weight, (kDa)	size/Å^3	PAA-0	PAA-0.5
lysozyme	14.6	19 × 25 × 43	378	436
BSA	69	40 × 40 × 140	115	175

CONCLUSIONS

The PSMC templating method was extended to the category of the anionic polyelectrolyte−nonionic surfactant mesomorphous complex. Because of the hydrogen bonding between anionic polyelectrolyte PAA and nonionic surfactant P123, the self-assembled mesomorphous PAA/P123 complex was first applied to synthesize hierarchically porous KIT-6 and SBA-15, which possessed both ordered mesopores (∼7 nm) and larger secondary nanopores (∼15−50 nm), and the long range order of mesopores was not perturbed by the embedded secondary nanopores, giving rise to a hierarchically porous single crystalline mesostructure. These kinds of hierarchically porous silica materials, with ordered mesopores larger than 7 nm and secondary nanopores of 15−50 nm, would be of interest in adsorption of large molecules, catalyst supports, and hard templates for porous functional materials.[35−37] Our experiments have proved that hierarchically porous silica KIT-6 exhibited enhanced loading capacity of biomacromolecules compared to the single-modal porous KIT-6.

EXPERIMENTAL SECTION

Chemicals. All chemicals were purchased and used without further treatment. Pluronic P123 (average molecular weight 5800, $EO_{20}PO_{70}EO_{20}$) was from Aldrich. Polyacrylic acid (PAA, average molecular weight 240 000, 25 wt % solution in water) was the product of Acros Organics. Hydrochloric acid (∼37 wt %) was the product of Tianjin Chemical Reagent Wholesale Company, China. TEOS and *n*-butanol were from Aladdin, China. BSA and lysozyme were products of Sigma-Aldrich.

Preparation of Hierarchically Porous Silica KIT-6. The typical synthesis condition of single-modal KIT-6 was based on the literature.[33] The synthesis of hierarchically porous silica KIT-6 was as follows: At 35 °C, 1.0 g pluronic P123 was added in 30 mL deionized water to form a solution, and a certain amount of 25 wt % PAA aqueous solution was added in the static state (the amount of PAA mentioned later in this paper refers to the amount of 25 wt % PAA aqueous solution), stirred for 10 min, and then 3.33 g of concentrated HCl (∼37 wt %) was put in. After 10 min of stirring, 1.0 g *n*-butanol was put in. After 30 min of stirring, 2.0 g of TEOS was added. The solution was kept in 35 °C water bath under stirring. After 24 h, the solution was put in an autoclave and was put in an oven at 100 °C for 24 h. The white precipitate was separated by filtration, purged with water, and dried at 50 °C. The template was removed by calcination at 550 °C for 6 h.

The samples synthesized with 3.33 g of concentrated HCl and different amounts of PAA were denoted as PAA-0, PAA-0.2, PAA-0.4 and PAA-0.5 (the number indicated the grams of the 25 wt % PAA solution used in synthesis), respectively. The sample synthesized with 0.5 g of PAA and 5.0 g of concentrated HCl was denoted as HCl-5.0.

Lysozyme Immobilization and BSA Adsorption. The operation procedures of enzyme and protein adsorption were same as those described in the previous literature.[20]

Characterization. The XRD patterns were measured on a Rigaku D/max-2500 diffractometer, with Cu Kα radiation working at 40 kV and 100 mA (λ = 0.15418 nm). A JEOL JSM7500F instrument was used for SEM observations. TEM images were obtained on a Philips Tecnai F20 microscope, working at 200 kV. The samples were dispersed in ethanol ultrasonically and copper grids were used to hold the sample. Nitrogen adsorption and desorption measurements were performed with a BELSORP-mini II sorption analyzer. The samples were pretreated for 6 h in nitrogen flow at 350 °C. The Brunauer−Emmett−Teller (BET) method was used to calculate the specific surface area and total pore volume (obtained at p/p_0 equals to 0.98). The data of adsorption branch were used to calculate the pore size distribution based on the Barrett−Joyner−Halenda method.

DOI: 10.1021/acsomega.8b03565
ACS Omega 2019, 4, 1443−1448

■ ASSOCIATED CONTENT

Supporting Information

The Supporting Information is available free of charge on the ACS Publications website at DOI: 10.1021/acsomega.8b03565.

XRD pattern, TEM images, SEM images, and so forth (PDF)

■ AUTHOR INFORMATION

Corresponding Author

*E-mail: chenth@nankai.edu.cn.

ORCID

Pingchuan Sun: 0000-0002-5603-6462

Tiehong Chen: 0000-0001-5162-9018

Notes

The authors declare no competing financial interest.

■ ACKNOWLEDGMENTS

This work was supported by NSFC (nos. 21773128, 21534005, and 21421001) of China.

■ REFERENCES

(1) Sun, M.-H.; Huang, S.-Z.; Chen, L.-H.; Li, Y.; Yang, X.-Y.; Yuan, Z.-Y.; Su, B.-L. Applications of hierarchically structured porous materials from energy storage and conversion, catalysis, photocatalysis, adsorption, separation, and sensing to biomedicine. *Chem. Soc. Rev.* **2016**, *45*, 3479−3563.

(2) Yang, X.-Y.; Chen, L.-H.; Li, Y.; Rooke, J. C.; Sanchez, C.; Su, B.-L. Hierarchically porous materials: synthesis strategies and structure design. *Chem. Soc. Rev.* **2017**, *46*, 481−558.

(3) Zhou, X.; Cui, X.; Chen, H.; Zhu, Y.; Song, Y.; Shi, J. A facile synthesis of iron functionalized hierarchically porous ZSM-5 and its visible-light photocatalytic degradation of organic pollutants. *Dalton Trans.* **2013**, *42*, 890−893.

(4) Fu, C.; Wang, S.; Feng, L.; Liu, X.; Ji, Y.; Tao, L.; Li, S.; Wei, Y. Hierarchically porous chitosan-PEG-silica biohybrid: synthesis and rapid cell adsorption. *Adv. Healthcare Mater.* **2012**, *2*, 302−305.

(5) Teng, W.; Bai, N.; Chen, Z.; Shi, J.; Fan, J.; Zhang, W.-x. Hierarchically porous carbon derived from metal-organic frameworks for separation of aromatic pollutants. *Chem. Eng. J.* **2018**, *346*, 388−396.

(6) Liang, H.-W.; Zhuang, X.; Bruller, S.; Feng, X.; Müllen, K. Hierarchically porous carbons with optimized nitrogen doping as highly active electrocatalysts for oxygen reduction. *Nat. Commun.* **2014**, *5*, 4973.

(7) Xu, M.; Feng, D.; Dai, R.; Wu, H.; Zhao, D.; Zheng, G. Synthesis of hierarchically nanoporous silica films for controlled drug loading and release. *Nanoscale* **2011**, *3*, 3329−3333.

(8) Li, N.; Niu, D.; Jia, X.; He, J.; Jiang, Y.; Gu, J.; Li, Z.; Xu, S.; Li, Y. Multiple gold nanorods@hierarchically porous silica nanospheres for efficient multi-drug delivery and photothermal therapy. *J. Mater. Chem. B* **2017**, *5*, 1642−1649.

(9) He, W.; Min, D.; Zhang, X.; Zhang, Y.; Bi, Z.; Yue, Y. Hierarchically nanoporous bioactive glasses for high efficiency immobilization of enzymes. *Adv. Funct. Mater.* **2013**, *24*, 2206−2215.

(10) Feinle, A.; Elsaesser, M. S.; Hüsing, N. Sol-gel synthesis of monolithic materials with hierarchical porosity. *Chem. Soc. Rev.* **2016**, *45*, 3377−3399.

(11) Sun, L.; Zhou, H.; Li, L.; Yao, Y.; Qu, H.; Zhang, C.; Liu, S.; Zhou, Y. Double soft-template synthesis of nitrogen/sulfur-codoped hierarchically porous carbon materials derived from protic ionic liquid for supercapacitor. *ACS Appl. Mater. Interfaces* **2017**, *9*, 26088−26095.

(12) Niu, D.; Ma, Z.; Li, Y.; Shi, J. Synthesis of core-shell structured dual-mesoporous silica spheres with tunable pore size and controllable shell thickness. *J. Am. Chem. Soc.* **2010**, *132*, 15144−15147.

(13) Esquena, J.; Nestor, J.; Vílchez, A.; Aramaki, K.; Solans, C. Preparation of mesoporous/macroporous materials in highly concentrated emulsions based on cubic phases by a single-step method. *Langmuir* **2012**, *28*, 12334−12340.

(14) Stein, A.; Rudisill, S. G.; Petkovich, N. D. Perspective on the influence of interactions between hard and soft templates and precursors on morphology of hierarchically structured porous materials. *Chem. Mater.* **2013**, *26*, 259−276.

(15) Estevez, L.; Dua, R.; Bhandari, N.; Ramanujapuram, A.; Wang, P.; Giannelis, E. P. A facile approach for the synthesis of monolithic hierarchical porous carbons-high performance materials for amine based CO2 capture and supercapacitor electrode. *Energy Environ. Sci.* **2013**, *6*, 1785−1790.

(16) Yang, H.; Liu, Q.; Liu, Z.; Gao, H.; Xie, Z. Controllable synthesis of aluminosilica monoliths with hierarchical pore structure and their catalytic performance. *Microporous Mesoporous Mater.* **2010**, *127*, 213−218.

(17) Cölfen, H. Single crystals with complex form via amorphous precursors. *Angew. Chem., Int. Ed. Engl.* **2008**, *47*, 2351−2353.

(18) Meldrum, F. C.; Cölfen, H. Controlling mineral morphologies and structures in biological and synthetic systems. *Chem. Rev.* **2008**, *108*, 4332−4432.

(19) Wang, J.-G.; Zhou, H.-J.; Sun, P.-C.; Ding, D.-T.; Chen, T.-H. Hollow carved single-crystal mesoporous silica templated by mesomorphous polyelectrolyte-surfactant complexes. *Chem. Mater.* **2010**, *22*, 3829−3831.

(20) Li, N.; Wang, J.-G.; Zhou, H.-J.; Sun, P.-C.; Chen, T.-H. Synthesis of single-crystal-like, hierarchically nanoporous silica and periodic mesoporous organosilica, using polyelectrolyte−surfactant mesomorphous complexes as a template. *Chem. Mater.* **2011**, *23*, 4241−4249.

(21) Shi, C.; Deng, S.; Wang, J.; Sun, P.; Chen, T. Hierarchically mesoporous silica single-crystalline nanorods with three dimensional cubic *Fm-3m* mesostructure. *J. Mater. Chem. A* **2013**, *1*, 14555−14561.

(22) Li, N.; Wang, J.-G.; Zhou, H.-J.; Sun, P.-C.; Chen, T.-H. Facile fabrication of hierarchically nanoporous SBA-1 nanoparticles. *RSC Adv.* **2012**, *2*, 2229−2231.

(23) Kong, L.; Liu, X.; Bian, X.; Wang, C. Silica nanocubes with a hierarchically porous structure. *RSC Adv.* **2012**, *2*, 2887−2894.

(24) Li, N.; Wang, J.-G.; Xu, J.-X.; Liu, J.-Y.; Zhou, H.-J.; Sun, P.-C.; Chen, T.-H. Synthesis of hydrothermally stable, hierarchically mesoporous aluminosilicate Al-SBA-1 and their catalytic properties. *Nanoscale* **2012**, *4*, 2150−2156.

(25) Shi, C.; Wang, W.; Liu, N.; Xu, X.; Wang, D.; Zhang, M.; Sun, P.; Chen, T. Low temperature oxidative desulfurization with hierarchically mesoporous titaniumsilicate Ti-SBA-2 single crystals. *Chem. Commun.* **2015**, *51*, 11500−11503.

(26) Zhu, Y.-P.; Qiao, S.-Z. Unprecedented carbon sub-microspheres with a porous hierarchy for highly efficient oxygen electrochemistry. *Nanoscale* **2017**, *9*, 18731−18736.

(27) Li, H.; Sun, Y.; Yuan, Z.-Y.; Zhu, Y.-P.; Ma, T.-Y. Titanium phosphonate based metal-organic frameworks with hierarchical porosity for enhanced photocatalytic hydrogen evolution. *Angew. Chem., Int. Ed. Engl.* **2018**, *57*, 3222−3227.

(28) Widenmeyer, M.; Anwander, R. Pore size control of highly ordered mesoporous silica MCM-48. *Chem. Mater.* **2002**, *14*, 1827−1831.

(29) Wan, Y.; Shi, Y.; Zhao, D. Designed synthesis of mesoporous solids via nonionic-surfactant-templating approach. *Chem. Commun.* **2007**, 897−926.

(30) Khutoryanskiy, V. V.; Mun, G. A.; Nurkeeva, Z. S.; Dubolazov, A. V. pH and salt effects on interpolymer complexation via hydrogen bonding in aqueous solutions. *Polym. Int.* **2004**, *53*, 1382−1387.

(31) Khutoryanskiy, V. V.; Dubolazov, A. V.; Nurkeeva, Z. S.; Mun, G. A. pH effects in the complex formation and blending of poly(acrylic acid) with poly(ethylene oxide). *Langmuir* **2004**, *20*, 3785−3790.

DOI: 10.1021/acsomega.8b03565
ACS Omega 2019, 4, 1443−1448

(32) Costa, T.; de Melo, J. S.; Miguel, M. d. G.; Lindman, B.; Schillén, K. Complex formation between a fluorescently-labeled polyelectrolyte and a triblock copolymer. *J. Phys. Chem. B* **2009**, *113*, 6205−6214.
(33) Kim, T.-W.; Kleitz, F.; Paul, B.; Ryoo, R. MCM-48-like large mesoporous silicas with tailored pore structure: Facile synthesis domain in a ternary triblock copolymer-butanol-water system. *J. Am. Chem. Soc.* **2005**, *127*, 7601−7610.
(34) Wang, Y.; Caruso, F. Mesoporous silica spheres as supports for enzyme immobilization and encapsulation. *Chem. Mater.* **2005**, *17*, 953−961.
(35) Soni, K.; Rana, B. S.; Sinha, A. K.; Bhaumik, A.; Nandi, M.; Kumar, M.; Dhar, G. M. 3-D ordered mesoporous KIT-6 support for effective hydrodesulfurization catalysts. *Appl. Catal., B* **2009**, *90*, 55−63.
(36) Shi, Y.; Guo, B.; Corr, S. A.; Shi, Q.; Hu, Y.-S.; Heier, K. R.; Chen, L.; Seshadri, R.; Stucky, G. D. Ordered mesoporous metallic MoO2 materials with highly reversible lithium storage capacity. *Nano Lett.* **2009**, *9*, 4215−4220.
(37) Pirez, C.; Caderon, J.-M.; Dacquin, J.-P.; Lee, A. F.; Wilson, K. Tunable KIT-6 mesoporous sulfonic acid catalysts for fatty acid esterification. *ACS Catal.* **2012**, *2*, 1607−1614.

DOI: 10.1021/acsomega.8b03565
ACS Omega 2019, 4, 1443−1448